

**ESTIMATION OF RUN-UP AMPLIFICATION
FACTORS FOR PENANG**

LIM YONG HUI

UNIVERSITI SAINS MALAYSIA

2017

ESTIMATION OF RUN-UP AMPLIFICATION FACTORS FOR PENANG

by

LIM YONG HUI

**Thesis submitted in fulfillment of the
requirements for the degree of
Master of Science**

June 2017

ACKNOWLEDGEMENT

First and foremost, I would like to express my sincerest appreciation to my supervisor, Associate Professor Dr. Teh Su Yean for her practical guidance, suggestions, patience and valuable comments throughout the process of completing this thesis. This accomplishment would not have been possible without her proficient supervision. I also extend my appreciation to Professor Koh Hock Lye for his advice on my research work. I would like to thank the Science Fund Grant #305/PMATHS/613418 from Ministry of Science, Technology and Innovation (MOSTI) for providing financial support for half of the research duration. In addition, I am grateful to be a recipient of MyMaster scholarship under the MyBrain15 program from the Ministry of Higher Education (MOHE). Further, I would like to acknowledge Pusat Hidrografi Nasional (PHN) and Jabatan Ukur dan Pemetaan Malaysia (JUPEM) for providing the high-resolution bathymetric and topographic data respectively. I am thankful for the support from the International Center of Theoretical Physics (ICTP) to participate in a high-performance computing workshop in October 2016. The superior academic surroundings in ICTP are exhilarating and mesmerizing. Moreover, in May 2016, I was funded by Institut Teknologi Bandung (ITB) to participate in a wave modeling workshop in Bandung, Indonesia. It has been a great learning experience and opportunity for me to participate in such a renowned research institution. The generous provision of facilities and space provided by the School of Mathematical Sciences (PPSM) and Institute of Postgraduate Studies (IPS), Universiti Sains Malaysia (USM) are greatly appreciated. I wish to thank my senior in USM, Tan Wai Kiat for teaching and guiding me at the beginning of my research. I am particularly grateful for the help and support provided by Tang

David throughout my research. Many friends have been delighting and supporting me during the journey of completing this thesis. Precisely, I am thankful to Kh'ng Xin Yi and See May Yen. Finally, I would like to express my deepest appreciation to my family for their bottomless support and unceasing encouragement throughout my study.

TABLE OF CONTENTS

Acknowledgement	ii
Table of Contents	iv
List of Tables	vii
List of Figures	viii
List of Symbols	xiii
Abstrak	xv
Abstract	xvii
CHAPTER 1 – INTRODUCTION	
1.1 Tsunami	1
1.2 Tsunami Simulation	2
1.3 Tsunami Early Warning System	3
1.4 Objectives of Thesis	5
1.5 Scope and Organization of Thesis	5
CHAPTER 2 – LITERATURE REVIEW	
2.1 Data Interpolation Studies	8
2.2 Run-up Amplification Factor Studies	11
2.3 Inundation Distance	17
CHAPTER 3 – PENANG BATHYMETRY AND TOPOGRAPHY	
3.1 Introduction	21
3.2 Interpolation Software	23
3.3 Interpolation Methods Comparison	24
3.3.1 Kriging	25
3.3.2 Radial Basis Function	27

3.3.3	Inverse Distance to Power	29
3.3.4	Demonstration of the Interpolation Methods	31
3.3.5	Characteristics of Test Method	33
3.4	Generation of Penang Map	39
3.4.1	Conversion of File Formats	39
3.4.2	Vertical Datum Adjustment	40
3.4.3	Inadequate Bathymetric Data	41
3.4.4	JUPEM Topographic Data of Four Domains	41
3.4.5	Bathymetric and Topographic Data Integration	41
3.5	Conclusion	42
CHAPTER 4 – RUN-UP AMPLIFICATION FACTORS		
4.1	Introduction	43
4.2	Numerical Model TUNA-RP	44
4.3	Scenario-Based Simulations	46
4.4	Results and Discussion	50
4.4.1	Incident Wave Heights	51
4.4.2	Orientations of Incident Wave	59
4.5	Comparison with 2004 Field Measurement Data	65
4.6	Conclusion	66
CHAPTER 5 – INUNDATION DISTANCES		
5.1	Introduction	67
5.2	Estimation of Inundation Distances	71
5.3	Worst Case Inundation	84
5.4	Comparison with 2004 Tsunami Simulation	86

5.5	Evacuation Analysis	89
5.6	Conclusion	93
CHAPTER 6 – CONCLUSION		
REFERENCES		98
APPENDIX		
LIST OF PUBLICATION		

LIST OF TABLES

		Page
Table 2.1	Roughness coefficients for different land use (Dickson et al., 2012)	19
Table 3.1	Interpolated values at points (0.5, 0, Zp1) and (1.5, 0, Zp2) using Kriging, Multiquadric-MQ, Thin Plate Spline-TPS and Inverse Distance to Power-IDP	32
Table 3.2	Statistical summary of digitized depth data from admiralty nautical chart	35
Table 3.3	Statistical analysis between measured depths and interpolated depths for data set in southern Penang Island	37
Table 3.4	Statistical analysis between measured depths and interpolated depths for overall bathymetric data sets	37
Table 4.1	Definition of symbols used in (4.1) to (4.3)	45
Table 4.2	Surveyed (Koh et al., 2009b) and simulated run-up heights in Penang	66
Table 5.1	Simulated and estimated inundation distances of different offshore wave heights for incoming wave from the west direction	80
Table 5.2	Simulated and estimated inundation distances of different offshore wave heights for incoming wave from the northwest direction	80

LIST OF FIGURES

		Page
Figure 3.1	JUPEM gridded topographic data in grey of four domains, I, II, III and IV with NHC scattered bathymetric data.	22
Figure 3.2	Transect of the surface produced by Kriging, MQ-Multiquadric, TPS-Thin Plate Spline and IDP-Inverse Distance to Power. The chosen points are marked by larger circles.	32
Figure 3.3	Interpolated results of four interpolation methods.	35
Figure 3.4	Admiralty nautical chart of south Penang (left) and interpolated result using Kriging (right).	36
Figure 3.5	Scattered-plots between measured depths and interpolated depths with the coefficient of determinations of (a) Kriging; (b) Multiquadric – MQ; (c) Thin Plate Spline –TPS; (d) Inverse Distance to Power – IDP for data set in southern Penang Island.	37
Figure 3.6	Scattered-plots between measured depths and interpolated depths with the coefficient of determinations of (a) Kriging; (b) Multiquadric – MQ; (c) Thin Plate Spline –TPS; (d) Inverse Distance to Power – IDP for overall bathymetric data sets.	38
Figure 3.7	Tidal levels and charted data.	40
Figure 3.8	Penang admiralty nautical chart (left) and interpolated map (right).	42
Figure 4.1	Regional map of Sumatra subduction zone and rupture areas of past great earthquakes. Red line is the interplate thrust that intersects the sea floor along the Sunda trench. Light yellow shaded area indicates the possible region where tsunami generated by earthquake will strike Northern Peninsular Malaysia. Yellow ellipses show the rupture of 1847, 1881, 1941 earthquakes (Jaiswal et al., 2008). Red circle represents the epicentre of 2004 earthquake and the dotted line marks the rupture zone (Jaiswal et al., 2008).	49

Figure 4.2	Direction of the incoming tsunami waves propagating from the west (a) and northwest (b) directions towards Penang Island.	50
Figure 4.3	Run-up amplification factors along the coast of Penang Island for the incoming wave direction from the west of Penang; red indicate 1 m incident wave height, blue indicate 2 m incident wave height and black indicate 3 m incident wave height.	52
Figure 4.4	Run-up amplification factors along the coast of Penang Island for the incoming wave direction from the northwest of Penang; red indicates 1 m incident wave height, blue indicates 2 m incident wave height and black indicates 3 m incident wave height.	53
Figure 4.5	Maximum horizontal inundation for the simulation of 1, 2 and 3 m incident wave heights, indicated in red, yellow and black respectively, with the incoming wave direction from the west of Penang Island.	54
Figure 4.6	Maximum horizontal inundation for the simulation of 1, 2 and 3 m incident wave heights, indicated in red, yellow and black respectively, with the incoming wave direction from the northwest of Penang Island.	55
Figure 4.7	Simulation setup for various slope angles, θ and incident wave heights, H . Figure not drawn to scale.	56
Figure 4.8	Regression plots between run-up amplification factors, R/H and incident wave heights, H for different slope angles of 2° , 15° , 30° and 45° .	57
Figure 4.9	Bathymetric transects with depth contours and their corresponding near-shore bathymetric profiles for some coastal regions of Penang Island.	58
Figure 4.10	Distribution of run-up amplification factors along the coastline of Penang Island for the incoming wave from the west (red) and northwest (black) directions of Penang Island with 1 m incident wave height.	60
Figure 4.11	Snapshots of wave propagations with velocity	61

vectors for simulation of incoming wave from the west direction of Penang Island. The time interval between each snapshot is 12 minutes.

Figure 4.12	Snapshots of wave propagations with velocity vectors for simulation of incoming wave from the northwest direction of Penang Island. The time interval between each snapshot is 12 minutes.	62
Figure 4.13	Comprehensive distribution of run-up amplification factors along the coastline of Penang Island integrated from the run-up amplification factors for west and northwest incoming tsunami wave directions towards Penang Island and three incident wave heights.	64
Figure 5.1	Ofunato City evacuation map with inundation depths in various colours and evacuation routes (Fraser et al., 2012).	69
Figure 5.2	Taro tsunami hazard map with three sections of tsunami wall in red (1958 section), black and yellow thick lines and tsunami gates in blue triangles and circles. The inundation extent of the 1986 Meiji is in thin red line and 1933 Shōwa tsunami is in thin blue line. Evacuation refuges are marked as red triangles and welfare centres as red circles. Source: Taro Town Disaster Prevention Office (Fraser et al., 2012).	70
Figure 5.3	Estimation of inundation distance (red) derived from run-up amplification factor and simulation of inundation distance (yellow) for offshore incident wave height of 2 m with incoming tsunami wave from the west direction.	74
Figure 5.4	Estimation of inundation distance (red) derived from run-up amplification factor and simulation of inundation distance (yellow) for offshore incident wave height of 3 m with incoming tsunami wave from the west direction.	75
Figure 5.5	Estimation of inundation distance (red) derived from run-up amplification factor and simulation of inundation distance (yellow) for offshore incident wave height of 2 m with incoming tsunami wave from the northwest direction.	76
Figure 5.6	Estimation of inundation distance (red) derived	77

from run-up amplification factor and simulation of inundation distance (yellow) for offshore incident wave height of 3 m with incoming tsunami wave from the northwest direction.

Figure 5.7	Snapshots of wave propagations with velocity vectors for simulation of incoming wave from the northwest direction with 3-m offshore wave height. The time interval between each snapshot is 8 minutes.	78
Figure 5.8	Snapshots of wave propagations with velocity vectors for simulation of incoming wave from the northwest direction with 1-m offshore wave height. The time interval between each snapshot is 8 minutes.	79
Figure 5.9	Comparison of estimated and simulated inundation distance with offshore incident wave height of 2 m (up) and 3 m (down) for incoming tsunami wave from the west direction.	81
Figure 5.10	Comparison of estimated and simulated inundation distance with offshore incident wave height of 2 m (up) and 3 m (down) for incoming tsunami wave from the northwest direction.	82
Figure 5.11	Fishing boats and villages at Kuala Sungai Burung (left) and Kuala Sungai Pinang (right).	82
Figure 5.12	Installed tsunami early warning sirens along the west and north coasts of Penang Island.	83
Figure 5.13	Comprehensive inundation map for Penang Island based upon 1, 2 and 3 m offshore wave heights. The blue dashed line indicates the possible further inundation at Gurney Drive for 3-m offshore incident wave height.	85
Figure 5.14	Simulated 2004 tsunami inundation distance (yellow) and comprehensive inundation map (red) based upon 1-m offshore wave height.	88
Figure 5.15	Estimated evacuation time needed for slow population (group of elderly) and fast population (individual adult) to evacuate to safe zone based on walking speed and inundation distance of worst case inundation with 3-m offshore incident wave height at the west coast of Penang Island.	90

Figure 5.16

Estimated evacuation time needed for slow population (group of elderly) and fast population (individual adult) to evacuate to safe zone based on walking speed and inundation distance of worst case inundation with 3-m offshore incident wave height at the north coast of Penang Island.

91

LIST OF SYMBOLS

X_{max}	maximum horizontal penetration of tsunami from the shoreline on a flat coastal topography
n	roughness coefficient
$\hat{Z}(\mathbf{s}_o)$	prediction values of interpolation method
\mathbf{s}_o	surface location for prediction values
$Z(\mathbf{s}_i)$	measured values of interpolation method
\mathbf{s}_i	surface location for measured values
N	number of neighbouring measured data points used for prediction
w_i	weights assigned to measured value
$\gamma_{i,j}$	variogram model measured at inter-point distance between all known data points
$\gamma_{i,o}$	variogram model measured at distance between a grid point to neighbouring measured data points
λ	Lagrange multiplier
$\varphi(r)$	basis function
r	radial distance from prediction point to measured point
$p(\mathbf{s}_o)$	polynomial term
m	order of basis function
a_o, a_1, a_2	coefficients for polynomial term
X	x- coordinate of interpolation point
Y	y- coordinate of interpolation point
c	smoothing factor
p	power parameter
D_i	distance between measured data point and unknown data point
Z_{p1}, Z_{p2}	interpolated values

p_i	predicted values in statistical expression
o_i	observed values in statistical expression
N_1	number of data values in statistical expression
t	time
x	distance for x- direction
y	distance for y- direction
η	free surface elevation measured from mean sea level
d	water depth below fixed datum
h	total water depth
g	gravitational acceleration
U	discharge fluxes in the x- direction
V	discharge fluxes in the y- direction
$\Delta x, \Delta y$	spatial grid size
Δt	time step
R	run-up height
H	offshore incident wave height
ET	evacuation time available
ETA	estimated tsunami arrival time
$ToNW$	technical or natural warning time
RT	reaction time of evacuees
IDT	Institutional Decision Time
INT	Institutional Notification Time

ANGGARAN FAKTOR-FAKTOR AMPLIFIKASI RAYAPAN BAGI PULAU PINANG

ABSTRAK

Tsunami mega yang melanda Malaysia pada 26 Disember 2004 memberi kesan kepada persisiran pantai barat laut Semenanjung Malaysia sepanjang 200 kilometer, dari Perlis hingga Selangor. Peristiwa malapetaka yang jarang ini telah menarik perhatian kerajaan Malaysia untuk mengambil langkah-langkah pengurangan risiko yang sesuai, termasuk pemindahan segera dan teratur. Untuk menentukan zon pemindahan, ketinggian gelombang tsunami yang tiba di pantai mesti diramalkan. Simulasi model mengambil masa yang terlalu lama untuk ramalan masa sebenar. Oleh itu, dalam tesis ini, suatu pendekatan yang menggunakan anggaran faktor-faktor amplifikasi rayapan untuk menganggar ketinggian rayapan dicadangkan sebagai cara yang mudah untuk mendapat anggaran pantas ketinggian rayapan melalui pendaraban faktor-faktor amplifikasi rayapan dengan ketinggian gelombang lepas pantai yang dikesan oleh sistem amaran awal tsunami. Simulasi model dijalankan dengan menggunakan model dalaman TUNA-RP untuk mendapat faktor-faktor amplifikasi rayapan dan jarak inundasi bagi Pulau Pinang. Bagi tujuan ini, data batimetri dan topografi resolusi tinggi bagi Pulau Pinang dari Jabatan Ukur dan Pemetaan Malaysia (JUPEM) dan Pusat Hidrografi Nasional (PHN) diinterpolasi dan diintegrasikan. Simulasi model menunjukkan bahawa faktor-faktor amplifikasi rayapan dipengaruhi oleh batimetri dan topografi di kawasan pesisiran pantai, ketinggian gelombang serta arah gelombang tsunami. Perbandingan antara ketinggian gelombang yang diukur bagi tsunami Andaman 2004 dan nilai-nilai rayapan yang dianggar berasaskan

faktor-faktor amplifikasi rayapan menunjukkan kesepakatan yang baik. Oleh itu, faktor-faktor amplifikasi yang diperolehi boleh menjadi alat yang berguna untuk penilaian awal bahaya tsunami yang pantas bagi Pulau Pinang. Faktor-faktor amplifikasi rayapan yang dianggarkan kemudian digunakan untuk mendapat anggaran pantas jarak inundasi di sepanjang persisiran pantai Pulau Pinang. Satu peta inundasi menyeluruh yang boleh digunakan bagi Pulau Pinang untuk penentuan pantas zon pemindahan dibentangkan. Jarak inundasi dan faktor-faktor amplifikasi rayapan yang dihasilkan dalam penyelidikan dijangka berguna kepada pengurus kecemasan dalam merancang pemindahan dan mengurus pembangunan persisiran pantai.

ESTIMATION OF RUN-UP AMPLIFICATION FACTORS FOR PENANG

ABSTRACT

The mega-tsunami that struck Malaysia on 26 December 2004 affected 200 kilometres of northwest Peninsular Malaysian coastline from Perlis to Selangor. This rare catastrophic event has awakened the attention of Malaysian government to take appropriate risk reduction measures, including timely and orderly evacuation. To determine the evacuation zones, the height of the tsunami waves arriving the shore must be predicted. Model simulations are too time-consuming for real time predictions. Therefore, in this thesis, an approach of applying run-up amplification factors to estimate the run-up heights is proposed as a simple way to obtain quick estimation of the run-up heights by multiplying the run-up amplification factors with the offshore incident wave heights detected by tsunami early warning system. Model simulations are performed using the in-house model TUNA-RP to obtain the run-up amplification factor and inundation distance for Penang Island. For this purpose, high resolution bathymetric and topographic data of Penang from Department of Survey and Mapping Malaysia (JUPEM) and National Hydrographic Centre (NHC) are interpolated and integrated. Model simulations show that the run-up amplification factors are mainly affected by the near-shore bathymetry and topography, incoming tsunami wave heights as well as the incoming wave directions. The comparison between measured tsunami wave heights for the 2004 Andaman tsunami and estimated run-up values derived from run-up amplification factors demonstrate good agreement. Hence, the derived amplification factors can be a useful tool for rapid preliminary assessment of tsunami hazards for Penang Island. The estimated run-up amplification factors are

then used to obtain rapid estimation of the inundation distances along the coastline of Penang Island. A comprehensive inundation map that could be used for Penang Island for rapid determination of evacuation zones is presented. The inundation distances and run-up amplification factors produced in this study would be useful to emergency managers for planning evacuation and managing coastal development.

CHAPTER 1

INTRODUCTION

1.1 Tsunami

Tsunamis are ocean waves with long wavelength of tens to hundreds of kilometres range and often travel with amplitude of less than one meter in the open sea and with speeds of around 700 – 800 km/h. They are commonly generated by the displacement of large volume of water during the occurrence of underwater tectonic activity such as underwater earthquakes, landslides on the sea floor or large volcanic eruptions. The surface of the Earth is constantly changing by diverging, converging and transforming the tectonic plates. Convergence between two plates causes the stresses between plates to build when they become stuck. When the stresses no longer hold, the sudden movement of the plates under the seafloor creates an undersea earthquake. The point of fault ruptures where this sudden movement of plates occur in both horizontal and vertical direction is called the epicentre. For the occurrence of noticeable tsunami, undersea earthquakes with magnitude of 7.5 or greater on the Richter scale is required (Singh et al. 2005). Although a large-magnitude undersea earthquake is necessary, the ocean floor must also be deformed vertically rather than horizontally in order to have large displacement of water. However, there might be exceptions when two plates slip horizontally past each other that triggers a large submarine landslide. Submarine landslides displace the water vertically and consequently generate a tsunami. As tsunamis travel from deep sea into the shallower water region approaching the coastal areas, their wave amplitude substantially increases,

while their wavelength and propagation speed decrease. This destructive feature of tsunamis is what causes great loss of lives and extensive damage in properties.

1.2 Tsunami Simulation

Tsunami model usually simulates the three phases of tsunami, namely tsunami generation, tsunami propagation as well as tsunami run-up and inundation by means of mathematical approaches. Tsunami is first generated by sources such as earthquake, submarine landslide or volcano followed by the tsunami wave propagation across the deep ocean to shallow water and finally inundates the dry land. If the wavelength of seabed deformation is much larger than the water depth, which is usually the case for co-seismic deformation, the free-surface displacement is assumed to be the same as seabed displacement (Kajiura, 1970). Typically, the Okada model (Okada, 1985) is applied to simulate the seabed deformation generated by undersea earthquake or volcanic dyke. The input parameters such as length, width, strike, dip and depth of a rectangular fault are needed to compute the free-surface displacement, tilts and strains. After initializing the tsunami wave generation, the propagation of tsunami wave is computed using the Shallow Water Equation (SWE) based on the water depth obtained from bathymetric data. Since the wavelength of tsunami is far larger than the water depth, tsunamis behave as shallow-water waves until the wave approaches the shore. As the tsunami waves approach the coastal areas, the linear approximation of shallow water equation is no longer valid because the water depth becomes shallower; thereby decreasing the wave velocity, shortening the tsunami wavelength and increasing the amplitude. The near shore tsunami propagation as well as run-up and inundation are then computed using the non-

linear shallow water equation (NSWE) coupled with the wetting-drying algorithm. Note that the run-up and inundation simulation requires high resolution of spatial grids of bathymetry and topography to obtain more accurate run-up and inundation distance. Tsunami simulation is required to estimate the tsunami wave heights, inundation distance and arrival times of specific tsunami source for tsunami early warning system. Tsunami model can be used to perform the real time simulation of tsunami propagation by reconstructing the initial tsunami waveform measured by buoy networks or pre-compute the run-up and inundation of worst case scenario to establish evacuation plans and community preparedness.

1.3 Tsunami Early Warning System

The tsunami waves triggered by an undersea earthquake off Aceh in Indonesia on 26 December 2004 have caused 52 deaths and more than 200 injured in Penang. The inadequate disaster preparedness system in Malaysia then has caught Malaysians unprepared for such a disaster. Since then, the Malaysian Government has taken various integrated measures to develop tsunami preparedness including the establishment of Malaysian National Tsunami Early Warning System (MNTEWS) to avoid similar tragedies. Tsunami early warning systems mainly use pre-computed tsunami scenarios based on the most active subduction zones historically. When a tsunamigenic earthquake occurs, the database of pre-computed tsunami scenarios are used to estimate the potential tsunami wave height along the coastlines. For real time tsunami forecasting, pre-computation is necessary because a detailed numerical simulation, particularly for the tsunami run-up and inundation phase, is too time consuming.

In the National Tsunami Early Warning Centre of Malaysia, the tsunami database is developed by considering tsunamigenic sources along the most active subduction zone at an interval of around 50 km with 5 different moment magnitudes, M_w (M_w 6.5, 7.0, 7.5, 8.0 and 8.5) and 4 different depths (0, 20, 40 and 60 km) (Chai et al., 2009). Three numerical models, namely TUNAMI-F1 (Tohoku University's Numerical Analysis Model for Investigation of Far-field tsunami, No. 1), TUNAMI-N2 (Tohoku University's Numerical Analysis Model for Investigation of Near-field tsunami, No. 2) and NAMI-DANCE version 4.7 are used. To estimate tsunami heights along the coast, Green's Law calculations are applied. Currently, the pre-computed tsunami database of MNTEWS contains more than 30,000 earthquakes scenarios (Chai et al., 2009).

Although such pre-computed data are valuable, they are designed for specific tsunamigenic earthquake sources. There might be some tsunami sources that are unrelated to earthquakes and subduction zones that are poorly defined, resulting in the unavailability of pre-computed tsunami scenarios. For example, an undersea earthquake with moment magnitude of M_w 9.0 – 9.5 is not considered in the pre-computed tsunami database of MNTEWS as well as the potential occurrence of submarine landslides at Bay of Bengal. Therefore, in this thesis, a fast alternative means of estimating tsunami hazard and impact on our shores is proposed to allow quick estimation of tsunami wave heights along the coast for a tsunamigenic event that might not have been prescribed in MNTEWS. Run-up amplification factor is applied to approximate the run-up height based upon the characteristics of incident wave and bathymetric slope. Run-up amplification factor is defined as the ratio of maximum run-up height to the tsunami height at shallow water (Satake,

1994). The use of run-up amplification factors to estimate expected run-ups on coasts offers great help to emergency managers trying to assess the hazard. The estimated run-ups on coasts can then be used to estimate the inundation distances. These estimated tsunami run-up heights and inundation distances are valuable in generating a detailed tsunami evacuation map to effectively evacuate the coastal communities.

1.4 Objectives of Thesis

The main objective in this research is to obtain run-up amplification factors and inundation distances for Penang Island. The specific objectives of this thesis include:

- a) To collate and interpolate the scattered bathymetric and topographic data of Penang Island.
- b) To obtain the run-up amplification factors along the coasts of Penang Island.
- c) To produce a comprehensive inundation map for Penang Island.

1.5 Scope and Organization of Thesis

Chapter 1 introduces the basic concepts and knowledge of tsunamis and tsunami early warning system. The simulation process of a tsunami event by a numerical model is briefly described. The motivation of using run-up amplification factor as a quick tool to estimate the run-up height on coast as well as the inundation distances is introduced. The objectives, scope and organization of this study are then listed.

Chapter 2 provides the review of literatures related to interpolation of bathymetric and topographic data, including the selection process of interpolation methods. This is followed by discussion of previous studies using amplification factors to investigate run-up and inundation along the coasts. The factors that influence inundation distance are then discussed.

The software used to perform the interpolation is introduced in Chapter 3. Several interpolation methods are briefly described, along with an example on interpolating points (Appendix). This is followed by the qualitative and quantitative comparison of the interpolation methods performance. The pre-processing and post-processing of interpolated bathymetric and topographic data are then depicted.

The TUNA-RP model used to simulate the run-up and inundation of tsunami is introduced in Chapter 4. The subduction zone and possible regions of tsunamigenic source are discussed, which leads to the selection of incoming tsunami wave directions for Penang Island. The computed run-up amplification factors along the coastline of Penang Island are then presented and discussed. The comprehensive run-up amplification factors that integrate the amplification factors for all incident wave heights and incoming wave directions are generated to provide useful insights. The obtained comprehensive run-up amplification factors are then used to estimate the run-up heights for the 2004 Andaman tsunami and the estimated result is compared with available field measurement data.

The estimated inundation distances derived by computed run-up amplification factors are presented in Chapter 5, along with the simulated inundation distances. The worst case inundation for different incident wave heights that integrates the estimated and simulated inundation distances for all possible tsunami wave directions is provided. The obtained worst case inundation is then used to compare with the 2004 tsunami inundation simulation result to observe the reliability of the inundation distance estimation. This chapter ends with a simple evaluation of evacuation time to provide insight into the applicability of inundation map. Chapter 6 will summarize the major conclusions of this study and recommend several directions for future work in mitigating tsunami hazard.

CHAPTER 2

LITERATURE REVIEW

2.1 Data Interpolation Studies

Spatial interpolation is primarily performed by environmental scientists to produce spatially continuous data in environmental sciences, for instance in climatology, soil moisture, bathymetry (seafloor surface) and topography (land surface) (Ruiz et al., 2016; Yao et al., 2013; Bello-Pineda and Hernández-Stefanoni, 2007; Erdogan, 2009), as precise and evenly spaced data are ambitious and expensive to obtain. They normally require such data as input grids for simulation or to make rationalized explanation. For tsunami simulation, the gridded seamless topo-bathy data are required as input data. The decrease in tsunami wavelength as it propagates towards the shore indicates the need to acquire finer bathymetric and topographic grids to preserve the resolution of wave and to obtain more detailed and precise estimation of run-up and inundation distances.

Sample size, data distribution and nature of data can affect the approximate calculation of spatial interpolation methods. Yao et al. (2013) demonstrated that the Empirical Bayesian Kriging (EBK) Regression Prediction or Regression-Kriging (RK), a geostatistical interpolation method, is the best interpolation method in generating the interpolated soil moisture data in the study. Bello-Pineda and Hernández-Stefanoni (2007) indicate that the Exponential Kriging interpolation method produces better result when compared to the Inverse Distance Function in creating the digital bathymetric model of Yucatan

submerged platform. Although spatial interpolation has been widely used to obtain regularly spaced bathymetric and topographic data for tsunami modelling, flood modelling, sea level change and sedimentation transport, there is no specific interpolation method that can produce best estimation for all types of bathymetric and topographic data.

Curtarelli et al. (2015) assessed the performance of three deterministic methods and a geostatistical interpolation method: (i) Inverse Distance Weighting, (ii) Local Polynomial Interpolation (LPI), (iii) Radial Basis Function (RBF) and (iv) Ordinary Kriging (OK) to obtain the gridded bathymetric data of Tucurui hydroelectric reservoir by means of ArcGIS Geostatistical Analyst toolbar—a geographic information system (GIS) software. The evaluation of interpolation methods showed that OK produces the highest accuracy data compared to the other interpolation methods although all methods produced visually similar results. The outcome of the bathymetry map was used for the reservoir optimization with operational monitoring.

Erdogan (2009) investigated the influence of data density on four interpolation methods: (i) Inverse Distance Weighting, (ii) Kriging, (iii) Multiquadric Radial Basis Function and (iv) Thin Plate Spline in generating the digital elevation models. ArcGIS 9.2 Geostatistical Analyst extension was used to interpolate the regularly sampled data, examine the accuracy of each interpolation methods on rocky hill and observe the effect of data density on the interpolation methods. The results revealed that Thin Plate Spline produces the smallest error and the best correlation coefficient for all data densities. On the other hand, Inverse Distance

Weighting produces the greatest overall error. For a lower sample density, the distribution of errors showed that most of the large errors were found at the rocky surfaces using all interpolation methods.

Yesuf et al. (2012) evaluated five interpolation methods, namely Kriging, Inverse Distance to Power, Natural Neighbour, Nearest Neighbour and Triangulation with linear interpolation algorithm, using Surfer 8.01 Golden Software to obtain the Lake Hardibo bathymetry map. The results showed that interpolated grids using Triangulation with Linear interpolation method gives a smaller error compared to other methods. Kubinský et al. (2014) and (2015) stated the use of Kriging in Surfer software to generate the 2×2 m grid size of water reservoir bathymetry with the verification of interpolated data quality performed by cross-validation method, but the details on the selection of interpolation method were not described and discussed in the paper.

As the choice of interpolation methods highly depend on the data set, it is crucial to carry out the accuracy evaluation to ensure the error of interpolated data is at minimum. Nevertheless, there is no standard method of accuracy assessment in selecting the interpolation method. Usually, researchers evaluate the accuracy of interpolation techniques by quantifying the interpolation errors via some statistical expressions using cross-validation method. Yesuf et al. (2012) performed the assessment on the quality of interpolation methods by calculating the errors using cross-validation method within Surfer. Curtarelli et al. (2015) used cross-validation implemented in ArcGIS to produce the Mean Absolute Error (MAE), Root Mean Square Error (RMSE) and coefficient of determination (R^2) of each

interpolation method. The frequently used error measurements in evaluating the accuracy of interpolation methods are Mean Error (ME), MAE, Mean Square Error (MSE) and RMSE (Li and Heap, 2008). In this thesis, the performance of interpolation methods is assessed by cross validation method, along with the error measurements: (i) ME, (ii) MAE, (iii) RMSE and (iv) R^2 .

2.2 Run-up Amplification Factor Studies

Early studies used the application of run-up amplification factor to correct the tsunami onshore run-up height. Satake (1994) was the first to express the ratio of the measured onshore tsunami run-up height to the computed tsunami height at a reference location in shallow water as the amplification factor. He compared the maximum amplitude at tide gauge calculated from the non-linear shallow water numerical computation to the observed run-up heights of the 1992 Nicaragua tsunami event because the inundation and run-up process was not included in the computation. The incapability to conduct the numerical simulation of tsunami run-up was due to the absence of an accurate and fine grid coastal topography and bathymetry of Nicaragua coast. Therefore, amplification factor was used to relate the computed tsunami heights in shallow water with observed run-up heights. Imamura et al. (1993), and Piatanesi et al. (1996) have also performed the tsunami simulations together with the used of amplification factor for the 1992 Nicaragua earthquake and tsunami event. The amplification factors obtained for the same event from Satake (1994), Imamura et al. (1993), and Piatanesi et al. (1996) do not show similarity. The selected locations where the near shore tsunami height was computed are different for the three simulations. Hence, it can

be perceived from these past studies that amplification factor depends strongly on the local topography.

Since then, amplification factor is also used for other purposes. Didenkulova et al. (2009) applied amplification factor to conduct the analysis of the shoaling effect of waves induced by high-speed Ferries in Tallinn Bay. The long waves (wavelengths up to 250 m) induced by ship wakes at depths of 10-20 m was analysed in the framework of shallow water theory. Didenkulova et al. (2009) recorded the wave heights 100 m offshore at water depth of about 2.7 m using an ultrasonic echosounder and the run-up heights on beach from 212 ship wakes events in Tallinn Bay. These experimental data were then used to find the run-up amplification factors, expressed as the ratio of maximum run-up height to measured wave height 100 m offshore. The experimental data demonstrated that run-up amplification factor decreases with the increasing incoming wave height. Didenkulova et al. (2009) explained this effect is caused by the wave breaking and dissipation in the turbulent bottom boundary layer.

In a more recent study, Sim and Huang (2015) constructed an experimental study of tsunami amplification on coastal cliff to examine the factors that may alter the amplification factors in the presence of coastal cliff. In the study, they defined the tsunami amplification factor as the ratio of tsunami height at onshore location of interest to the reference tsunami height at offshore location. They listed the main reasons to select the reference location of measuring the offshore wave height near to coastline as the difficulties to obtain fine grid of coastal bathymetric and topographic data and the availability of tide gauges in shallow water. The

experiment was designed to examine and test the effect of four different incident wave heights and five different onshore cliff slopes on amplification factors. Five conclusions were drawn from the experimental results:

1. The existence of coastal cliff vastly increases the water elevation before the cliff.
2. For a given incident wave height, the amplification factor generally increases with steeper cliff slope.
3. For a given cliff slope, the amplification factor increases with smaller incident wave height.
4. For a given incident wave height and cliff slope, the amplification factor increases as the onshore location recording the water level approaches the cliff.
5. For the largest incident wave height, the amplification factor is smaller than the rest, possibly due to wave breaking and other nonlinear phenomena.

On the other hand, some studies on the amplification factors were designed to obtain the analytical maximum run-up solutions over a planar beach. Keller and Keller (1964) related the amplification factor to beach width, wave number of incident wave and Bessel's functions to determine the maximum run-up for monochromatic waves on sloping beach using linear shallow water equations. Several run-up laws that relate run-up height and offshore wave height were then derived empirically and analytically for different incident waveforms (Synolakis, 1987; Tadepalli and Synolakis, 1994, Pelinovsky and Mazova, 1992). These run-up laws have been used to provide rapid estimate of the run-up heights on planar

beach. However, in real bathymetry, the applicability of these analytical run-up laws is restricted. Min et al. (2011) presented a rapid projection method to predict the tsunami run-up heights for the east Korea by combining numerical simulation and analytical run-up solutions that involve the use of amplification factor derived by Keller and Keller (1964). The two-dimensional nonlinear shallow water equations were first used to simulate the tsunami wave propagation from the open sea to water depth of 10 m with 1 km rough resolution bathymetry. A vertical wall was placed at the 10 m depth to record the water wave oscillations. The incident and reflected waves of the water wave oscillations were then separated. The incident and reflected waves can be separated easily if the seabed near the vertical wall is nearly constant. However, if the vertical wall is located on an inclined bathymetry, the Hankel functions were used. Carrier-Greenspan transformation (Carrier and Greenspan, 1958) was used to transform two one-dimensional first order nonlinear shallow water equations to a single second order linear wave equation with the rationale that incident wave far from the shoreline contains only small nonlinear effects. The linear wave equation for water displacement was then transformed to the general solution of shoreline water displacement using Fourier transformation. The spectra amplitude of incident wave was then re-computed on the shore using the general solution of water displacement. General solution of water displacement of the shoreline together with the amplification factor is then used to estimate the run-up heights. The amplification factor for the near-shore of East (Japan) Sea is around 2 to 2.2. The applicability of the combined method of two-dimensional numerical model and one-dimensional analytical run-up theory was checked with the observed run-up heights of the 1983 tsunami event in the East (Japan) Sea. However, there are several limitations of the combined method

presented in the paper. The run-up on shore was calculated using one-dimensional analytical run-up theory, when in fact the numerical tsunami run-up simulation considers two-dimensional geometry in the real seabed. This means that the two-dimensional wave effects such as refraction and focusing close to the shore are neglected. In addition, the near-shore bathymetry profile and the vertical wall are approximated as planar beach with the same slope. This assumption of approximating the real bathymetry by planar beach can affect the run-up process and hence vary the result.

In order to obtain reasonable estimates of maximum shoreline water level for global tsunami hazard in a simpler and faster way, Løvholt et al. (2012) used the method of amplification factors to estimate the maximum shoreline water level based on characteristics of incident wave (earthquake fault width, leading trough or crest and dip angle) and bathymetric slopes. The amplification factors were obtained from plane wave numerical simulations on idealized two-dimensional bathymetry transects by relating wave elevation measured by time series gauges at water depth of 50 m to the maximum shoreline water level at 0.5 m water depth. The amplification factors were then stored in a lookup tables and used to multiply with the highest wave elevation at time series gauges obtained from tsunami propagation simulation to acquire the estimation of maximum shoreline water level. The highest wave elevations at each gauge were extracted from the tsunami propagation simulation performed by two horizontal dimensions (2HD) model known as GloBouss (Pedersen and Løvholt, 2008). The estimated maximum water levels obtained from the combination of tsunami propagation simulation and amplification factors for Sri Lanka, Barbados and NW-Philippines were compared

with two-dimensional inundation model known as ComMIT (Titov and Synolakis, 1995; 1998). The result indicated slightly conservative estimates, which is 20% higher than the estimated maximum water levels obtained by ComMIT. In the paper, the method of computing amplification factors does not include two-dimensional near-shore wave behaviours such as focusing, refraction and diffraction since the plane wave theory is used. Moreover, the idealized bathymetry transects used to calculate the amplification factors were piece-wise linear planar beach. In an actual tsunami event, the variations of coastal bathymetry and topography cannot be represented as a plane beach. The near-shore bathymetry characteristics play a key role in influencing the run-up process.

Ward and Day (2008) performed near-shore tsunami propagation, run-up and inundation simulation by tracking accelerating tsunami balls that represents tsunami energy. Several two-dimensional simulation cases that based on beach slope and wave period were performed and the run-up amplification factors (the ratio of run-up height to initial wave height) were computed using the run-up heights obtained in the simulations. The computed run-up amplification factors for short, intermediate and long waves are 0.43, 0.63 and 1.17 respectively. They found that the empirical run-up formula that relate to amplification factor applied by Chesley and Ward (2006) will always return amplification factor of more than one while the amplification factors obtained by Ward and Day (2008) can be less than one when the wave breaking is significant. In fact, Chesley and Ward (2006) recognized that the empirical run-up formula used is independent of wave period or beach slope and it cannot be applied in every case. Ward and Day (2008) argued that the run-up height should be viewed as a random variable because it

varies with many factors including beach slope, wave period and initial wave height. For this reason, this thesis intends to obtain run-up amplification factors for Penang Island by simulating two-dimensional tsunami near-shore propagation, run-up and inundation on real bathymetry and topography based upon incident wave height and wave direction.

2.3 Inundation Distance

Inundation map allows emergency planners to evaluate the potential damage and lives loss at coastal areas. It is important as the fundamental step for emergency planners to take proper response and appropriate mitigation measures. Inundation distance is usually predicted to assist evacuation planners to assess the number of population at risk, evacuation routes and evacuation time required. Further, the regions that are most vulnerable to the tsunami threats can be determined from the inundation prediction and destructions from past tsunami event.

Tsunami inundation distance is mainly influenced by the coastal topography and land use. Local topography with low-lying land is likely to have longer inundation distance while steeper topography experiences shorter inundation distance. Goto et al. (2012) conducted the field measurement of run-up and inundation distance at Sendai Plain of the 2011 Tohoku-oki tsunami. The field measurement results showed that the inundation distance is longer at flat coastal topography in Sendai (around 4000 m) than the inundation distance at steep coastal topography in Yamamoto (around 2000 m). On the other hand, Goto et al. (2012) stated that land use type such as buildings, infrastructure, rivers and highway is a factor that affects the horizontal extent of inland inundation. These different types of land

use are able to restrict the tsunami wave from penetrating further inland to a certain degree by dissipating tsunami wave energy. The field study depicted that there is a negative correlation between run-up and inundation at Sendai Plain. This is probably due to high dependence of the run-up and inundation on the local topography. For steeper topographic slope, the run-up height was higher with shorter inundation distance. While on the flat surface, the inundation distance was long and the run-up height was low. However, in a densely populated area that consists of buildings and infrastructures, the inundation distance was shorter with lower run-up height because the tsunami energy might have been reduced by the artificial structures.

Chandrasekar et al. (2012) investigated the correlation between inundation and coastal geomorphology at Kanyakumari District, India. He claimed that the coastal inundation extent mainly depends on the coastal geomorphic setting. The study revealed that estuarine coast is favourable to the tsunami inundation. Shallow coastal area was found to endure high tsunami inundation, while elevated coastal land impedes the tsunami wave to inundate much of the coastal area. In the 2004 Indian Ocean tsunami event, estuaries, river inlets and low-lying topography experienced larger inundated areas and more death tolls along the South Eastern Coast of India (Chandrasekar and Ramesh, 2007). Although shallow coast is vulnerable to tsunami, land cover such as elevated coastal sand dunes and coastal forests can act as barriers to reduce the tsunami wave energy. Sim et al. (2013) conducted experimental study on the effectiveness of coastal sand dunes in reducing the tsunami energy. He reported that coastal sand dunes could successfully mitigate the impacts of tsunami if the height of sand dunes is of

the same order of magnitude as the incoming tsunami wave height and the gaps between dunes are larger than the near-shore tsunami wavelength. However, in reality, the gaps between dunes are unlikely to be larger than the near-shore tsunami wavelength. Although the tsunami wavelength close to shore is shorter than the offshore tsunami wavelength, the near-shore tsunami wavelength is still possibly much longer than the dune gaps. It is more likely to have sand dunes with height greater than the incoming tsunami wave height for small tsunami or storm surge. Therefore, high coastal sand dunes can defend against tsunami with low incoming tsunami wave height. Forbes and Broadhead (2007) stated that all types of coastal forest including mangroves, beach forests and plantations are able to dissipate the tsunami energy, reduce the water flow velocity and thereby restrict inundation extent.

Dickson et al. (2012) stated that for a flat surface, the extent of inundated area barely depends on coastal topography but on surface roughness. The UK Tsunami Initiative developed an inundation model where the inundation distance is calculated based on the tsunami wave height at shoreline and the friction factors that resists the tsunami from flowing rapidly (Dickson et al., 2012). The friction factors are determined from roughness coefficient that is based on the type of land use. Table 2.1 shows the roughness coefficients for respective land use types.

Table 2.1: Roughness coefficients for different land use (Dickson et al., 2012)

Land Use Type	Roughness Coefficient, n
Mud flats, ice, open fields without crops	0.015
Built-up areas	0.035
City centre	0.100
Forests, jungles	0.070
Rivers, lakes	0.007

The maximum horizontal penetration of tsunami from the shoreline on a flat coastal topography, X_{\max} can be computed as below:

$$X_{\max} = \frac{0.06H_0^{4/3}}{n^2} \quad (2.1)$$

where H_0 is the tsunami wave height at shore and n is the roughness coefficient obtained from Table 2.1. It should be noted that this method is only applicable for coastal areas with flat surface.

From the review above, it can be seen that the type of land use, land cover and coastal topography are the main factors affecting the inundation distance. However, Fernando et al. (2008) and Dewi (2010) stated that the inundation extent could also be affected by bathymetry, orientation of incoming wave, near shore wave height and wavelength, tide level and tsunami magnitude. Some of these factors, namely coastal topography and bathymetry, orientation of incoming wave and near shore wave height, are considered in this thesis.

CHAPTER 3

PENANG BATHYMETRY AND TOPOGRAPHY

3.1 Introduction

The accuracy of tsunami run-up and inundation simulation depends significantly on the resolution of bathymetric and topographic data. High resolution bathymetric and topographic data is essential, particularly at coastal areas, to provide a more precise simulation of tsunami run-up and inundation. However, high resolution gridded bathymetric and topographic data sets of Malaysia are not freely available online. The seamless integration of high resolution bathymetric and topographic data is even scarcer. Typically, the topographic and bathymetric data are collected and processed separately by different agencies. In Malaysia, the bathymetry data are generally collected by the National Hydrographic Centre (NHC) of the Royal Malaysian Navy for ship navigation purposes while the topographic data are collected by the Department of Survey and Mapping Malaysia (JUPEM) for land mapping purposes. For this research study on Penang, the higher resolution coastal bathymetry data are obtained from NHC while the higher resolution topography data are obtained from JUPEM. Figure 3.1 depicts the multiple domains in which the topography and bathymetry data are obtained. As shown in Figure 3.1, the bathymetric data from NHC are sparse and scattered. Hence, they require further processing—via data interpolation—for integration with JUPEM’s topographic data, which are given in regularly spaced grid systems (Gesch and Wilson, 2002). Several common interpolation methods for bathymetry and topography data are tested and the most suitable method is selected for developing a grid spacing of 1 arc-second (30 m) bathymetric and topographic

surface data of Penang. The process of integrating and interpolating topographic and bathymetric data can be a challenging task owing to the disparity in data availability and format as well as the vertical datum. The data processing and interpolation methodology used to obtain uniform and consistent bathymetry and topography data for TUNA-RP simulation will be illustrated in this chapter.

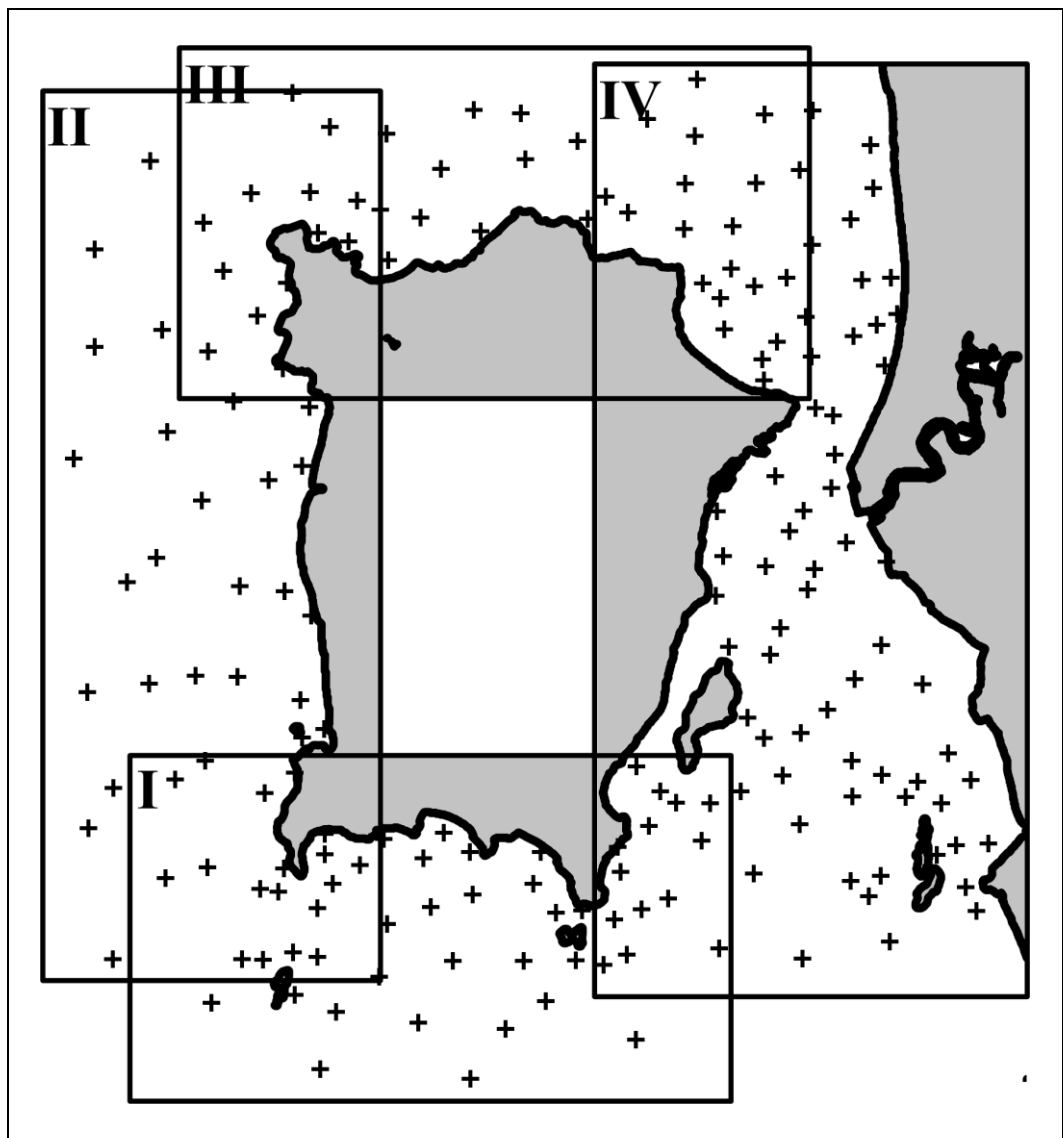


Figure 3.1: JUPEM gridded topographic data in grey of four domains, I, II, III and IV with NHC scattered bathymetric data.

3.2 Interpolation Software

Data in fixed interval grid system are usually required for numerical simulations but most existing data are sparse and scattered since precise and consistent data measurement can be time-consuming and financially demanding. To convert data in a scattered form to a regularly spaced grid, interpolation is often employed to estimate the unknown values from the existing known data source values.

The available interpolation functions in Surfer, a commercial software developed by Golden Software Inc., are used to convert the low density, scattered NHC bathymetric data into 1 arc-second high resolution regularly gridded bathymetric data and to obtain the full topographic map of Penang. Surfer is a contouring, gridding and 3D surface mapping software that interpolates irregularly spaced XYZ data source into a regularly spaced data (Surfer[®] 11 Quick Start Guide, 2012). The contour maps and surface plots in Surfer require a regularly spaced data points in grid files (.grd). The irregularly spaced XYZ data source can be transformed into a regularly spaced grid data values by employing an interpolation method in Surfer. Several interpolation methods available in Surfer are tested and the most suitable interpolation method is chosen to interpolate the bathymetric data from NHC and topographic data from JUPEM.

There are twelve different interpolation methods in Surfer, namely (i) Inverse Distance to Power, (ii) Kriging, (iii) Minimum Curvature, (iv) Polynomial Regression, (v) Triangulation, (vi) Nearest Neighbour, (vii) Modified Shepard's Method, (viii) Radial Basis Functions, (ix) Natural Neighbour, (x) Moving Average, (xi) Data metrics and (xii) Local Polynomial. Surfer is able to

interpolate up to one billion XYZ data points and produce grids with up to hundred million nodes. The interpolation methods in Surfer can be classified by two groups, exact interpolators and smoothing interpolators. Exact interpolators can honour data points exactly when the data point lies directly on a grid node. It is plausible that the data points are not honoured exactly even if exact interpolators are applied. Smoothing interpolators can be applied when the existing sample data measurements are uncertain in accuracy. They do not honour the data points even if the data falls exactly on the grid node but they can produce a smoother surface by varying the weighting factors. According to Erdogan (2009), the most popular and commonly used interpolation methods in generating the gridded topographic and bathymetric surfaces are (i) Kriging, (ii) Radial Basis Function, specifically Multiquadric (MQ) and Thin Plate Spline (TPS) and, (iii) Inverse Distance to Power (IDP). Therefore, these interpolation methods are selected for the interpolation tests, the results of which will be presented in the next section.

3.3 Interpolation Methods Comparison

There have been many studies on the assessment of spatial interpolation methods performance in generating Digital Elevation Model (DEM) and Digital Bathymetry Model (DBM) (Erdogan, 2009; Bello-Pineda and Hernández-Stefanoni, 2007; Curtarelli et al., 2015). However, there is no best interpolation method that can be used in a particular type of data sets or applications. The best method is only applied for a specific situation (Isaaks and Srivastava, 1989). The performance of interpolation methods is primarily affected by factors such as data density, data distribution and nature of data (Li and Heap, 2008). Hence, it is